SIX YEARS OF METOP-A AVHRR SEA SURFACE TEMPERATURE

Anne Marsouin, Pierre Le Borgne, Gérard Legendre, Sonia Péré

Météo-France/DP/Centre de Météorologie Spatiale
BP 50747, 22307 Lannion, France

Abstract

The Ocean and Sea Ice Satellite Application Facility (OSI SAF) has been producing global Sea Surface Temperature (SST) from METOP-A AVHRR since July 2007. The SST operational processing and the validation scheme have been unchanged during 6 years.
The global validation results against in situ measurements are good and stable with time. By night, the SST mean error is -0.05 K and the error standard deviation is 0.45 K, by day, these values are respectively 0.09 K and 0.58 K. Regional and seasonal errors, due to the limitations of the multi-spectral algorithms, have been observed. Seasonal statistics have been calculated on a global regular 5-degree grid for a 5-year period to review the main errors and their characteristics.

INTRODUCTION

The Ocean and Sea Ice Satellite Application Facility (OSI SAF) of EUMETSAT has been producing global Sea Surface Temperature (SST) data from the METOP-A Advanced Very High Resolution Radiometer (AVHRR) since July 2007. The OSI SAF products are now widely used, for instance by the Met Office OSTIA SST analysis, and sometimes considered as a reference when merging SST products from various satellites.
METOP-A SST validation results against in situ measurements are good when calculated globally, but regional and seasonal errors are observed. Assessing these errors is important for the users and for the development of the future OSI SAF METOP-B AVHRR chain.
This text summarizes the SST operational processing (section 2) and the validation scheme (section 3) and describes the validation results (section 4).

SST OPERATIONAL PROCESSING

The OSI SAF METOP-A SST chain includes the following main steps:

a) preprocessing: the full resolution radiometric data are ingested in near real time for each METOP 3-minute granules. The threshold based MAIA cloud mask (Lavanant, 2007), is calculated on these data.

b) cloud mask control: several tests are applied on each pixel that concern the local gradient, the local SST, occurrence of aerosol, occurrence of ice. Each test is defined by two values associated to a test indicator varying from 0 to 100. The range limited by the two values corresponds to a potential problem (test indicator in]0,100[), one side of the range corresponds to a critical problem (test indicator=100) and the other side to no problem (test indicator=0). The test indicators are then averaged to obtain the so-called cloud mask indicator. Furthermore, if one test indicator is equal to 100 , the cloud mask indicator is equal to 100

c) Multi-spectral algorithm:
The SST is calculated by classical multi-channel formulas, where the coefficients have been derived from simulations. A radiative transfer model has been applied to a data base of cloud free radio soundings and the coefficients have been calculated by multilinear regressions on simulated

brightness temperatures (Francois et al, 2002). The “NL” algorithm (equation 1) is used by day and the “T37_1” algorithm (equation 2) by night.

NL $SST = a\,T_{11} + (b\,T_{CLI} + c\,S_\theta)(T_{11} - T_{12}) + d + e\,S_\theta + corr$ (1)

T37_1 $SST = (a + b\,S_\theta)\,T_{37} + (c + d\,S_\theta)(T_{11} - T_{12}) + e + f\,S_\theta + corr$ (2)

with T_{11} T_{12} $T_{3.7}$ brightness temperatures at 11.0, 12.0 and 3.7 μm, respectively (Celsius).
T_{CLI} climatological SST value (Celsius)
a,b,c,d,e,f coefficients calculated by multilinear regressions (table 1)
corr correction term obtained on the first validation results (table 1)
$S_\theta = 1/\cos(\theta) - 1$ θ is the satellite zenith angle

	a	b	c	d	e	f	corr
NL	**0.99052**	**0.06641**	**1.16321**	**1.26512**	**0.16400**	**-**	**0.23**
T37_1	**1.01867**	**0.02109**	**0.68858**	**0.33056**	**1.02351**	**1.27303**	**0.13**

***Table 1*: coefficients of the METOP-A SST algorithms, NL by day and T37_1 by night, with all temperatures expressed in Celsius.**

A Saharan Dust Index (SDI) correction term is calculated as a quadratic function of the SDI values derived from SEVIRI data (Merchant *et al.,* 2006), for 0.1<SDI<0.8. This correction depends on the algorithm used. No corrections are made when there is no SEVIRI observations. In these conditions, the aerosol contaminated cases are flagged using the aerosol information in the NWC SAF cloud mask or the NAAPS Aerosol Optical Depth (US NAVY, 2003).

d) quality level: a quality level is associated to each pixel with the following values: 0 : unprocessed, 1 : cloudy , 2: bad, 3: suspect, 4: acceptable, 5 : excellent. The quality level value is derived from the cloud mask indicator and the satellite zenith angle. Pixels considered as dubious after the cloud mask control (i.e. cloud mask indicator equal to 100) are labeled “cloudy”.

e) operational product fabrication: the full resolution SST products directly result from the previous processing steps. The remapped products, 12 hourly synthesis on a global 0.05° regular grid (GLB) and 2km stereopolar product over European seas (NAR), are obtained with similar principles. For the GLB product, all SST data available in a 12-hour time are aggregated, giving a priority to high quality levels, nighttime cases and low satellite zenith angles, then the resulting field is remapped onto the global grid. For the NAR product, the aggregation considers the pixels located in the NAR area and with 9-hour time, then the remapping is onto the NAR grid.

.

For more details on the chain, see Le Borgne et al., 2007 or EUMETSAT, 2013.

VALIDATION SCHEME

The operational validation of the OSI-SAF SST is based on the Matchup Data Base (MDB). The MDB collects in situ SST measurements from ship, moored or drifting buoys, available through the Global Telecommunication System (GTS) and the coincident full resolution satellite information, within 3 hours from the in situ measurement. The satellite information (calculated SST, brightness temperatures and reflectances) is extracted in a 21x21 pixel box centred on the measurement location providing the coverage of the box by clear pixels is larger than 10%. The MDB includes the in situ measurements (platform ID +SST + auxiliary measures) and all the variables used in METOP SST processing

The MDB is built with a 5 day delay to insure a good collection of the in situ data through the GTS.

The validation statistics are based on the exploitation of the MDB, as follows:

- Drifters only are considered.
- Nighttime and daytime algorithms are considered separately.
- A blacklist of dubious buoys is used to eliminate erroneous measurements. This blacklist is based

on the OSI SAF SST processing, corresponding to several satellites: METOP-A, NOAA-18 or NOAA-19, METEOSAT and GOES-E (Marsouin et al., 2010). In addition, cases where the absolute value of the difference between the in situ measurement and the climatology exceeds 5 K are eliminated

With the above principles, the SST error is defined as the SST at the central pixel of the validation box minus the in situ measured SST, which is closest in time.

The statistics are calculated at various temporal resolutions (1 day, 10 days, 1 month, for routine validation and on longer time periods, for studies) on the global area or on the areas defined for OSI SAF SST validation (figure 1).

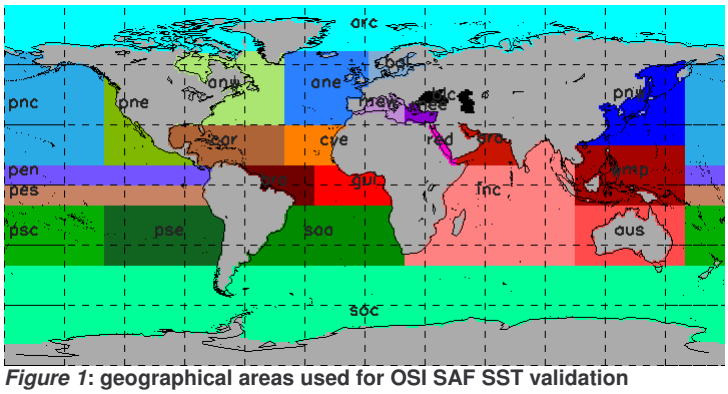

***Figure 1*: geographical areas used for OSI SAF SST validation**

RESULTS

Most of the validation results presented here have been obtained on a 6-year period (1 July 2007 to 31 July 2013), some of them concern a shorter 5-year period (1 October 2007 to 30 September 2012). The statistics have been calculated on the cases having a quality level in 3-4-5, which is the range recommended to users, except in section 4.1 where results are given per quality level.

Global error

METOP-A SST error statistics have been calculated globally over 6 years (table 2). When considering the cases with quality levels 3-4-5, good results are obtained by night, with a negligible mean error of -0.05 K and a standard deviation of 0.45 K. The daytime results, mean error of -0.09 K and standard deviation of 0.58 K, are worse, due to a less efficient NL algorithm (2 channels instead of 3 channels by night) and locally to a possible diurnal warming effect.

Quality level	night time			day time		
	bias (K)	st dev (K)	nb cases	bias (K)	st dev (K)	nb cases
3-4-5	-0.05	0.45	424461	0.09	0.58	535957
5	-0.01	0.37	153827	0.13	0.51	218279
4	-0.04	0.45	132877	0.08	0.57	201054
3	-0.11	0.52	137757	0.05	0.69	116624
2	-0.23	0.63	52387	-0.15	0.75	37459

***Table 2:* METOP-A SST error, global statistics from 1 July 2007 to 31 July 2013. "bias" is the mean error, "st dev" the error standard deviation and "nb cases" the number of cases. Column 1 gives the selected quality level values.**

The global statistics on cases with quality levels 3-4-5 are rather stable during the 6-year period (figure 2 left); except that the nighttime mean error shows a small trend, decreasing from 0. to -0.1 K. The number of cases, by night and by day, decrease from 2011 on-wards. This is not related to the validation scheme, but to a decrease of the drifting buoys number and of their observations, clearly seen on the In situ SST Quality Monitor (iQuam), http://www.star.nesdis.noaa.gov/sod/sst/iquam/

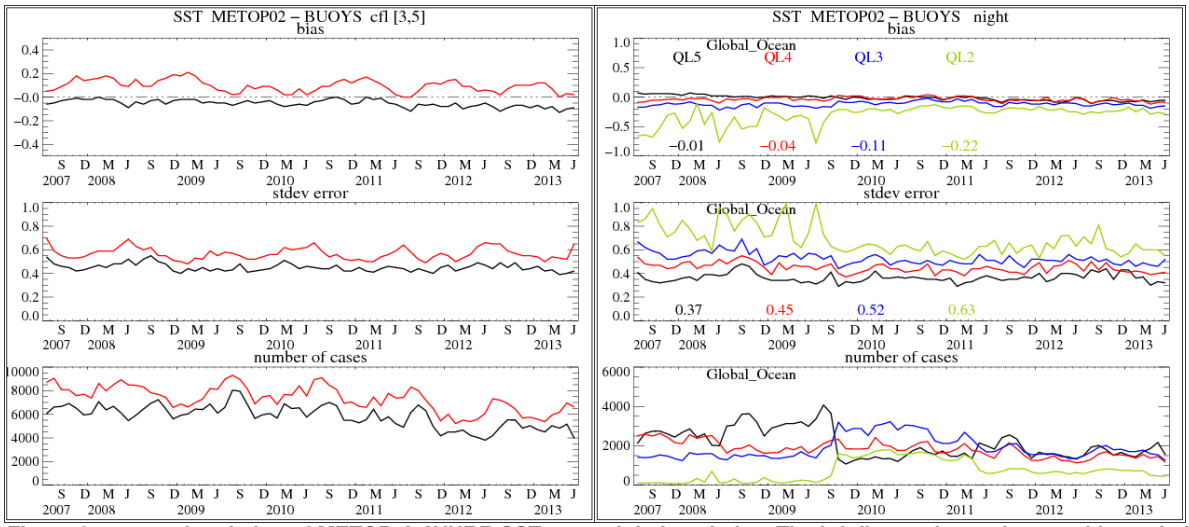

Figure 2: **temporal variation of METOP-A AVHRR SST error global statistics. The left figure shows the monthly statistics on cases with quality levels 3-4-5, for nighttime (black) and daytime (red). The right figure shows the nighttime monthly statistics, per quality level: 5 (black), 4 (red), 3 (blue), 2 (yellow). Each figure shows the mean error (top plot), the error standard deviation (middle plot) and the number of cases (bottom plot) as a function of time.**

Global statistics have been calculated for each quality level value (table 2). When the quality level decreases from 5 to 2, the SST mean error decreases and the error standard deviation increases, from 0.37 K to 0.63 K by night and from 0.51 K to 0.75 K by day. These variations are mainly due to more aerosol or cloud contaminated pixels entering into the statistics. The statistics per quality level are also reasonably stable with time (figure 2 right), except for the numbers of cases, which vary because of NAAPS data. The lack of NAAPS data decreases the aerosol indicator and, consequently, the quality level. NAAPS data dissemination was stopped in September 2009 and restored in June 2010, but with a longer delay. The METOP-A SST chain schedule was modified in May 2011 to cope with the longer delay, without reaching the full availability of NAAPS data, as in years 2007-2009.

Decrease of the nigttime mean error

In order to investigate the nighttime mean error decrease (figure 2 left), the monthly mean error has been plotted for a few validation areas, which do not present important regional errors (section 4.3). The decrease is observed in the northern hemisphere (figure 3 left), but not in the southern hemisphere (figure 3 right). This north-south difference is unexplained, so far.

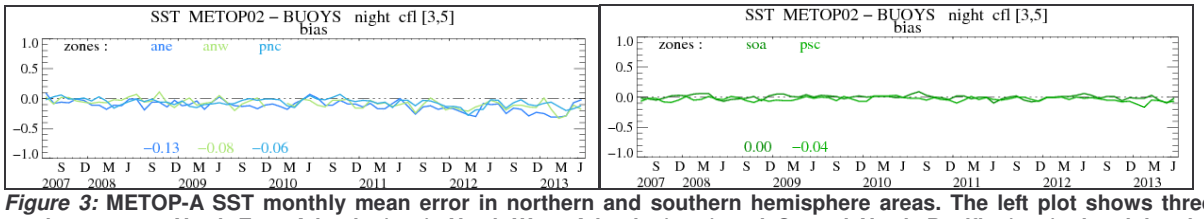

Figure 3: **METOP-A SST monthly mean error in northern and southern hemisphere areas. The left plot shows three northern areas, North-East Atlantic (ane), North-West Atlantic (anw) and Central North Pacific (pnc), the right plot shows two southern areas: South Atlantic (soa) and Central South Pacific (psc). The areas are presented in figure 1.**

Regional errors

Regional and seasonal errors have been commonly observed in satellite derived SST products (Le Borgne et al, 2007, Le Borgne et al, 2010; Marsouin et al, 2010). In the present study, these errors have been studied on a 5-year MDB (1 October 2007 to 30 September 2012). The validation statistics have been calculated on a global regular 5-degree grid, separately on four quarters: Q1 (Jan-Feb-Mar), Q2 (Apr-May-Jun), Q3 (Jul-Aug-Sep), Q4 (Oct-Nov-Dec). Only the cases with quality level in 3-4-5 have been used and the 5-degree boxes having less than ten cases have been rejected.

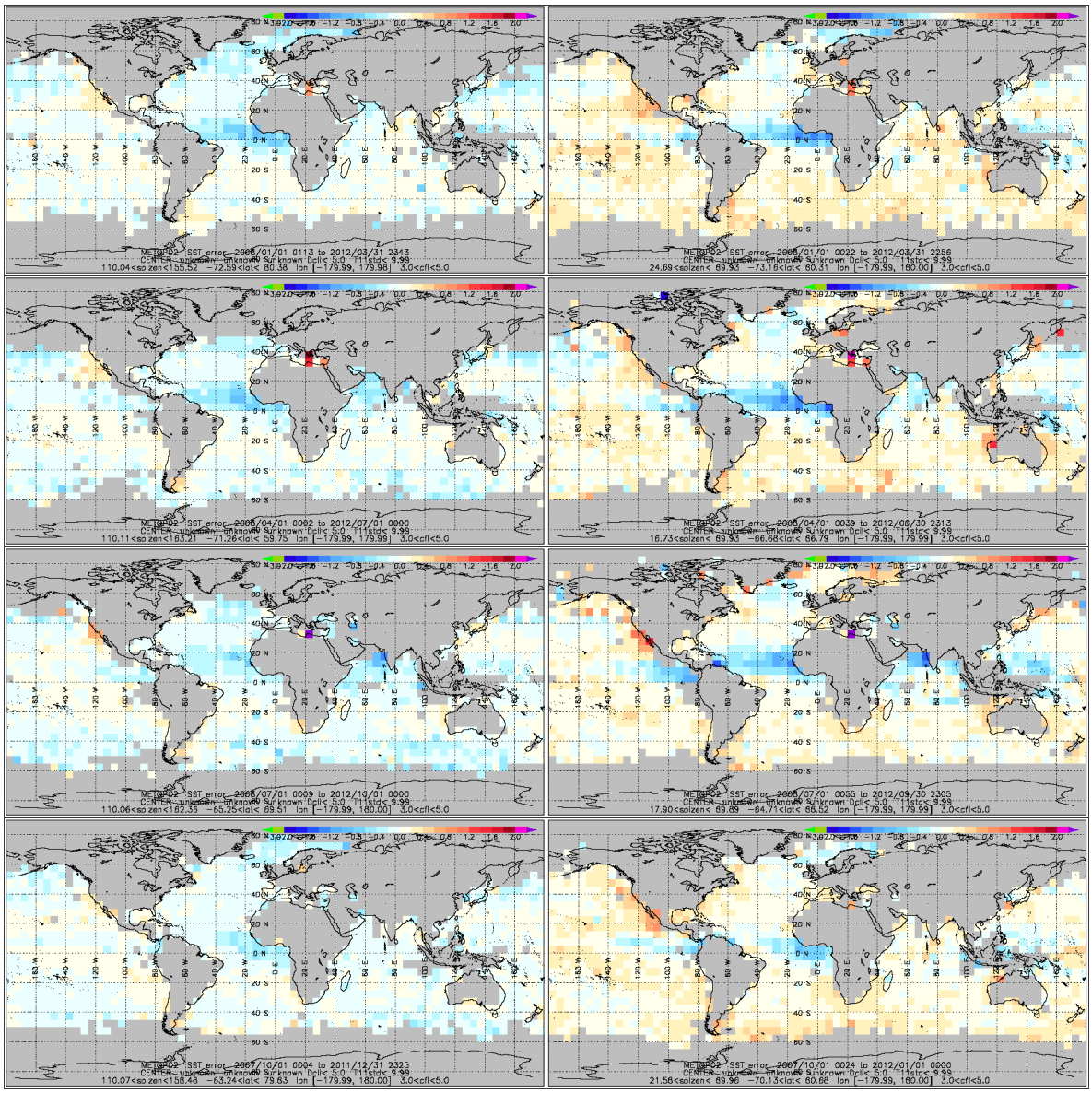

Figure 4: **METOP-A SST quarterly mean error on a 5-year MDB (October 2007 – September 2012). The nighttime errors are shown on the left figures, the day time errors on the right figures. The four rows correspond to the four quarters: Q1 (Jan-Feb-Mar), Q2 (Apr-May-Jun), Q3 (Jul-Aug-Sep), Q4 (Oct-Nov-Dec). The blue-red color scale corresponds to values from -2 K to 2K, with values lower than -2 K in green and values higher than 2 K in magenta.**

The quarterly mean errors for night and day are presented in figure 4. High errors (in absolute value) are generally observed in the same places for night and day, but they are usually higher by day, likely due to a less efficient SST algorithm (2 channels by day instead of 3 channels by night).

The most critical problem occurs in Tropical Atlantic with negative errors up to -1 K. The error pattern varies seasonally: from January to May, the error is high (in absolute value) and covers a wide area centered along 10N, from October to December, the error is lower and covers a smaller area in the Gulf of Guinea. The error amplitude also varies from year to year (figure 5 left).

Positive errors are observed by night and by day, off California (Pacific Ocean), nearly all year round. However theses errors may be undetected, since the number of drifting buoys in this area is sometimes low (figure 5 right).

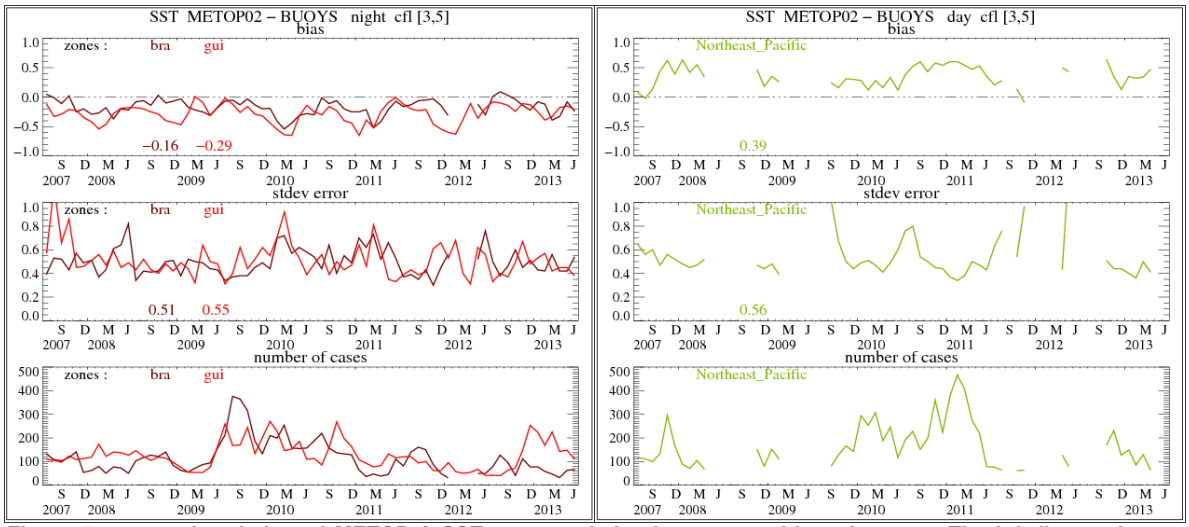

Figure 5: **temporal variation of METOP-A SST error statistics in some problematic areas. The left figure shows the nighttime monthly statistics in Equatorial Atlantic, Brazil (bra) and Gulf of Guinea (gui), the right figure the daytime monthly statistics in North East Pacific (pne). Each figure shows the mean error (top plot), the error standard deviation (middle plot) and the number of cases (bottom plot) as a function of time. The areas are presented in figure 1.**

Other problems are observed, which are less important, in terms of error amplitude, geographical or temporal coverage:

- negative error by night and by day, in Arabian Sea, from April to September,
- negative error by day, in the Warm Poll, nearly all year round,
- positive error, by night and by day, off Argentina in Southern Atlantic ,nearly all year round, the error being rather low and covering a small area

The regional errors are mainly due to the limitations of the multi-spectral algorithms, which cannot cope with full variability of the atmospheric profiles. Merchant et al, 2009A, has demonstrated that SST derived from METOP-A AVHRR data by NL algorithm do present errors in Tropical Atlantic, North of Indian Ocean and Warm Pool. These algorithm errors may be removed or reduced by two approaches: optimal estimation (Merchant et al, 2008, Merchant et al 2009B) or algorithm correction simulated with a radiative transfer model and forecast atmospheric profiles (Le Borgne et al, 2011A). These studies deal with NL algorithm, but they question the multi-spectral algorithm principles, so similar results are expected with the T37_1 algorithm.

An algorithm correction is operational, since August 2011, in the OSI SAF geostationary SST chain (GOES-E and METEOSAT). This correction efficiently reduces SST errors in Tropical Atlantic, off California and off Argentina, see figure 6 and Le Borgne et al, 2011B for more details.

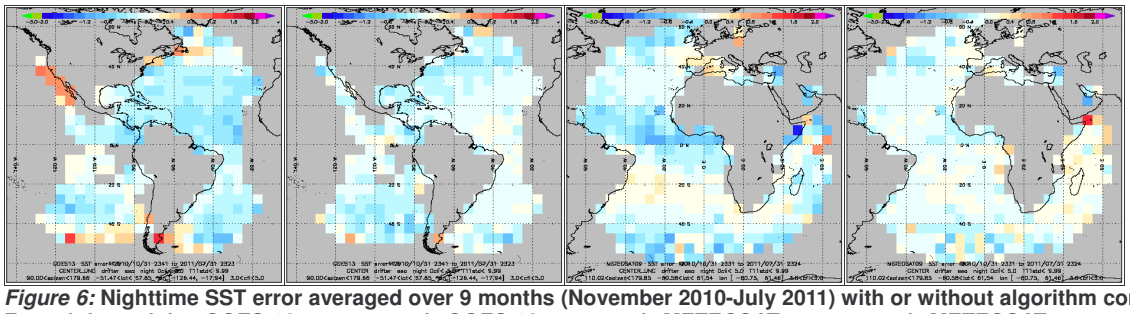

Figure 6: **Nighttime SST error averaged over 9 months (November 2010-July 2011) with or without algorithm correction. From left to right, GOES-13 uncorrected, GOES-13 corrected, METEOSAT uncorrected, METEOSAT corrected, with same color scale as figure 4.**

The future OSI SAF METOP-B chain will include an algorithm correction. A prototype chain ingesting METOP-A AVHRR data has been run for one year and most regional biases are corrected (Le Borgne et al, 2013).

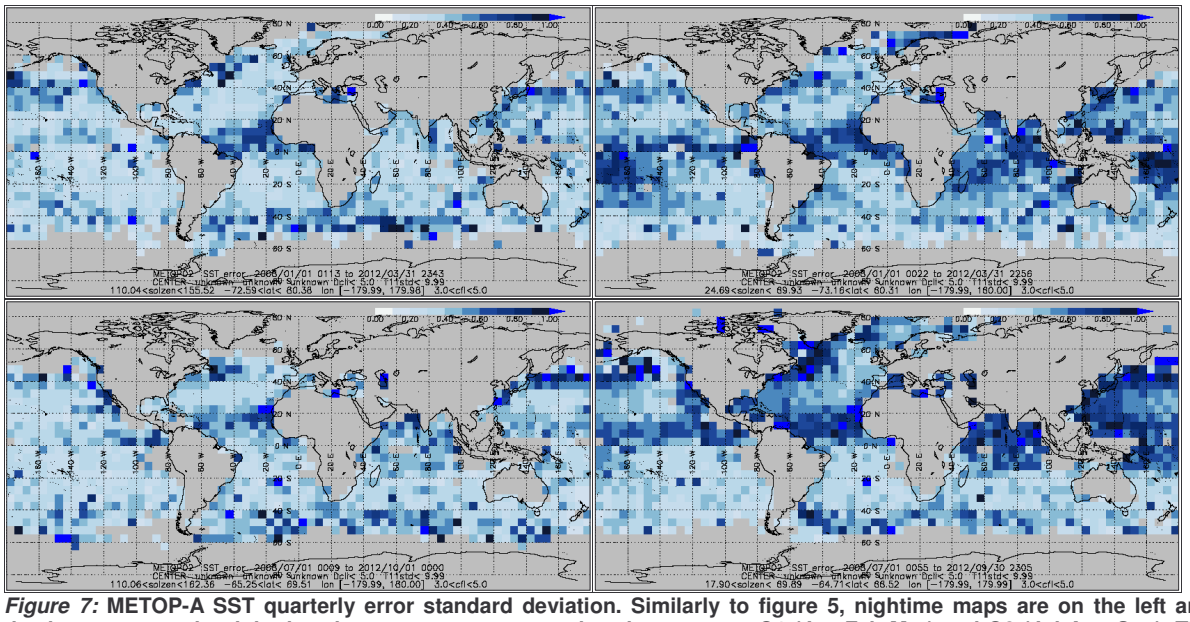

Figure 7: **METOP-A SST quarterly error standard deviation. Similarly to figure 5, nighttime maps are on the left and daytime maps on the right, but the two rows correspond to the quarters: Q1 (Jan-Feb-Mar) and Q3 (Jul-Aug-Sep). The white-blue color scale corresponds to values from 0 to 1 K, with values higher than 1 K in a brighter blue..**

Figure 7 presents the nighttime and daytime error standard deviations (STDE) for two quarters, Q1 (Jan-Feb-Mar) and Q3 (Jul-Aug-Sep). The STDE do not vary much during the year and the two quarters are representative of the observed variations. Consistently with the global statistics, the STDE values are higher by day than by night.

Regional variations are observed, mainly:

- High STDEs are associated to the Tropical Atlantic negative mean errors, but this is not true for other regions of significant mean error.
- High STDEs are observed in high SST gradient regions, such as Gulf Stream and Kuro-Shivo, which is physically consistent.
- By day, high STDE are observed in wide areas: the North of Indian Ocean all year round and in the North West Pacific from April to August.

The STDE maps have been less investigated than the mean error maps, the regional patterns remain to be understood.

CONCLUSION

The OSI SAF has been producing global SST from METOP-A AVHRR since July 2007, with the same operational processing and validation scheme during 6 years. The SST is calculated by a three channel (11µm, 12µm, 3.7 µm) algorithm by night and a two channel (11µm, 12µm) algorithm by day.

The global validation results against in situ measurements are good, better by night than by day, and stable with time. On the cases with quality levels 3-4-5 (which is the range recommended to users), the SST mean error is -0.05K and the error standard deviation is 0.45K by night, these values being respectively 0.09K and 0.58K by day. The quality level associated to each SST value is informative: when the quality level decreases from 5 to 2, the SST error standard deviation increases from 0.37 K to 0.63 K by night and from 0.51 K to 0.75 K by day.

Regional errors, mainly due to the limitations of multi-spectral algorithms, have been observed on the whole period: The major problem is the negative errors, up to -1 K, frequently observed in Tropical Atlantic. Other significant errors are positive errors off California and off Argentina, negative errors in Arabian Sea and in the Warm Pool. These errors are higher (in absolute value) by day than by night, they vary seasonally in terms of intensity and spatial extension. The description of these errors is

important to inform METOP-A AVHRR SST users and to prepare the future OSI SAF METOP-B chain, which will include an algorithm correction.

REFERENCES

EUMETSAT (2013), Low Earth Orbiter Sea Surface Temperature Product User Manual, version 2.3, June 2013,.http://www.osi-saf.org/index.php

Francois C., Brisson, A., Le Borgne, P. and Marsouin, A. (2002), "Definition of a radiosounding database for sea surface brightness temperature simulations: application to sea surface temperature retrieval algorithm determination", *Remote Sensing of Environment*, **81**, 309-326.

Lavanant, L., (2007) Operational cloud masking for the O&SI SAF global METOP SST production, proceedings of the 2007 EUMETSAT conference, Amsterdam, The Netherlands, September 2007.

Le Borgne, P., G. Legendre and A. Marsouin (2007), Operational SST retrieval from METOP/AVHRR, proceedings of the 2007 EUMETSAT conference, Amsterdam, The Netherlands, September 2007.

Le Borgne, P., Roquet, H. and Merchant, C., (2011A). Estimation of sea Surface Temperature from the SEVIRI, improved using numerical weather prediction, *Remote Sensing of Environment* 115, 55–65.

Le Borgne, P., A. Marsouin, F. Orain and H. Roquet (2011B), New OSI SAF SST geostationary chain, Validation Results, proceedings of the 2011 EUMETSAT conference, Oslo, Norway, September 2011.

Le Borgne, P., G. Legendre, A. Marsouin, S. Péré, H. Roquet (2013), SST From Polar Orbiter Satellites (METOP, NOAA and NPP); New OSI SAF Products and developments, this conference.

Marsouin, A., P. Le Borgne, G. Legendre, S. Péré, (2010), Homogeneous validation scheme of the OSI SAF sea surface temperature products, proceedings of the 2010 EUMETSAT conference, Cordoba, Spain, September 2010.

Merchant, C.J., O. Embury, P. Le Borgne and B. Bellec, (2006). Saharan dust in nighttime thermal imagery: Detection and reduction of related biases in retrieved sea surface temperature, *Remote Sensing of Environment*, **104**,15-30.

Merchant, C. J., A.R. Harris, H. Roquet and P. Le Borgne (2009A), Retrieval characteristics of non-linear sea surface temperature from the Advanced Very High Resolution Radiometer. *Geophys. Res. Lett*, 36, L17604, doi:10.1029/2009GL039843.

Merchant C. J., P. Le Borgne, H. Roquet and A. Marsouin (2009B), Sea surface temperature from a geostationary satellite by optimal estimation, *Remote Sensing of Environment*, 113 (2), 445-457.

US NAVY, (2003), Description of NAAPS (Navy Aerosol Analysis and Prediction System) Global Aerosol Model), http://www.nrlmry.navy.mil/aerosol_web/Docs/globaer_model.html .